SNPP and N20 VIIRS thermal emissive bands calibration comparison using the GEO-LEO double difference method

Tiejun Chang,[a*] and Xiaoxiong Xiong[b]
[a] Science Systems and Applications, Inc., Lanham, MD 20706
[b] Sciences and Exploration Directorate, NASA/GSFC, Greenbelt, MD 20771

Abstract. The VIIRS instruments onboard the SNPP and NOAA-20 satellites have identical spatial resolutions and the same spectral bands. Similar prelaunch tests and identical on-orbit calibration algorithms established the foundation for their consistent Earth measurements. Calibration assessment and consistency comparisons are useful to maintain their performance and measurement accuracy. Simultaneous nadir overpasses (SNO) between two satellites are commonly used for a direct calibration comparison between sensors. However, there are no SNO between SNPP and NOAA20. Hence, a reference sensor or Earth measurements are normally used to bridge the comparison. As a reference, we focus on the Advanced Baseline Imager (ABI) onboard the GOES-R series spacecraft and its application to the SNPP and NOAA-20 VIIRS comparison. GOES16 and GOES17 are the first two satellites of the GOES-R series and were launched on November 19, 2016 and March 12, 2018, respectively. Their operational positions are on the equator with longitudes of 75.2° West over land and 137.2° West over ocean, respectively. The ABI is the primary imaging instrument of these spacecrafts for the Earth's weather, oceans, and environment, with observations (every 10 minutes) that provide vast data for GEO- Low Earth orbit (LEO) and LEO-LEO comparisons utilizing it as an intermediate reference sensor. VIIRS and ABI have spectrally matched bands and can have simultaneous measurements over any selected site every day. The simultaneous measurements over the same site also have various scan angles. These features provide advantages for a VIIRS-to-ABI comparison. The spectral response function difference between instruments, sites selected, and view angles will have effects on the instrument measurements. Their impacts on the calibration comparison, including the use of double differences, will be discussed. By collecting VIIRS measurements over a large range of view angles, the view angle effect will also be investigated. The collection of an ample amount of data provides an advantage for statistical analyses and potential big data applications to sensor calibration assessments. This method can also be applied to other sensor calibration comparison and performance assessments, such as GOES16 and GOES17 ABI, and Terra and Aqua MODIS.

Keywords: GOES-16, GOES17, ABI, VIIRS, inter-comparison

***** Corresponding author e-mail: tiejun.chang@ssaihq.com

1 Introduction

The Visible Infrared Imaging Radiometer Suite (VIIRS) is a key instrument onboard Suomi National Polar-orbiting Partnership (SNPP) and NOAA20 (N20) satellites on Low Earth orbit (LEO). SNPP was launched on October 28, 2011, and N20 was launched on 18 November 2017 and in the same orbit as SNPP [1-4]. VIIRS provides the science and user communities with high quality product. Accurate calibration is essential to achieve precise specifications and maintain high quality of the data products. The assessment of radiometric calibration stability is necessary to enhance calibration accuracy. VIIRS thermal emissive band (TEB) on SNPP and on N20 have the same design and specifications, and TEB calibration is performed using same algorithm. The comparison between VIIRS on SNPP and on N20 is an important factor in their calibration and performance assessments. Since both spacecrafts are in the same orbit with different equator passing time, there is no simultaneous nadir overpass (SNO) to be used as a direct calibration comparison [5]. Hence, a common reference is needed to enable sensor comparison.

Geostationary satellites (GOES)-16 and GOES17 were launched on November 19, 2016 and March 1, 2018, respectively. The Advanced Baseline Imager (ABI) is the primary instrument onboard both spacecrafts and is used to image the Earth's weather and environment. [6-9]. The ABI instrument provides a full disk Earth image every 10 minutes. Their near-continuous and simultaneous observations provide a great advantage as a reference for inter-sensor calibration assessments.

This paper focuses on the methodology development and application of comparison between the SNPP/VIIRS and N20/VIIRS TEB using GOES17 ABI TEB as reference. Section 2 provides the background of VIIRS and ABI instruments. Section 3 presents the methodology development. Section 4 presents the results via the differences between the two VIIRS instruments using double difference.

2 Background

2.1 Instruments

VIIRS is onboard the SNPP and N20 Low Earth orbit (LEO) satellites, which have the same orbit but different equator passing time. VIIRS has 14 reflective bands covering 0.4-2.2 μm and 7 emissive bands covering 3.7-12 μm. The spatial resolution at nadir is 750m for the 16 moderate resolution radiometric bands (M bands) and 375 m for the 5 imaging bands (I bands) [1, 2]. Each M band consists of 16 detectors. Bands M1-11 are reflective bands and M12-16 are thermal emissive bands. Each I band consists of 32 detectors. Bands I1-I3 are reflective bands and I4 and I5 are thermal emissive bands. SNPP/VIIRS and N20/VIIRS have the same design, specification, and same calibration algorithm. VIIRS TEB use nonlinear response function for calibration and on-orbit calibration uses on-board blackbody (BB) and deep space as calibrators.

GOES16 and GOES17 are the first two satellites of NOAA Geostationary Operational Environmental Satellites (GOES-R) series. GOES16 was launched on November 19, 2016. The spacecraft reached the GOES East position (longitude of 75.2° West) by December 11, 2017. It was declared fully operational on December 18, 2017. GOES17, launched on March 1, 2018, became operational as GOES-West (longitude of 137.2° West) on February 12, 2019 [6-9].

ABI is the primary payload aboard the GOES-R satellites. It provides high spatial and temporal resolution Earth imagery through 16 spectral bands at the visible, NIR, and IR wavelengths. Among the 16 spectral bands, bands 7 to 16 are infrared channels covering the 3.9 to 13.3 μm range. The ABI TEB spatial resolutions are 2 km in their full-disk image products. ABI produces full-disk Earth images every 10 minutes (GOES16 ABI produced full-disk images every 15 minutes before April 2, 2019). For the GOES16 and GOES17 ABI, the spectral coverages of their TEB are almost identical, and the same calibration algorithms are applied using data from their on-board calibrators.

2.2 Inter-sensor comparison for TEB

Intercomparisons between the Level 1B (L1B) brightness temperatures (BT) of the SNPP/VIIRS and N20/VIIRS TEB can be used to assess calibration accuracy and detect anomalies in straightforward fashion. Sensor inter-comparisons using Earth measurements have been discussed previously in the literature [5, 10-12]. SNO is a method for the inter-satellite sensor comparison of the TEB. The SNO method has also been applied to ABI TEB assessments using MetOp-B's IASI and the S-NPP Cross-track Infrared Sounder (CrIS) [13]. The double difference method has also been applied to compare GOES instruments using reference sensors such as MODIS and VIIRS [14]. Calibration sites such as qDCC, Dome Concordia (Dome-C) in Antarctica, Lake Tahoe, ocean buoys, and various sites can also be used for thermal stability assessments. The GOES sensors image the full Earth disk and provide near-continuous observations and feasibility of near-simultaneous comparison, which is advantageous as reference for inter-sensor comparisons.

3 Methodology and data processing

3.1 Spectral band matching

This work focuses on the comparison between VIIRS M TEB bands and ABI, and the double difference application between SNPP/VIIRS and N20/VIIRS. Figure 1 shows the GOES17 ABI and SNPP VIIRS TEB spectral response function. When selecting the matched bands, their spectral coverage and the Earth scene spectrum should be considered. The effect of spectral coverage difference between two sensors on their comparison depends on the Earth scene spectrum. In a spectral range with many spectral features or on a slope of the scene spectrum, the spectral difference can have a large impact on the ABI-VIIRS comparison. These spectral difference effects can be reduced when comparing SNPP/VIIRS and N20/VIIRS by using the double difference method. The typical ocean BT spectrum, modeled using MODTRAN, is plotted as a reference in the Figure. There are 7 pairs of matched bands selected for this work, as shown in table 1. VIIRS M15 has its center wavelength between of ABI bands 13 and 14. Since ocean BT spectrum is flat in that spectral range, two matched pairs are selected as M15-B13 and M15-B14. Similarly, the bands M16-B14, M16-B15, M12-B7, and M13-B7 are also paired for comparison, even though the spectral coverages do not have good matching.

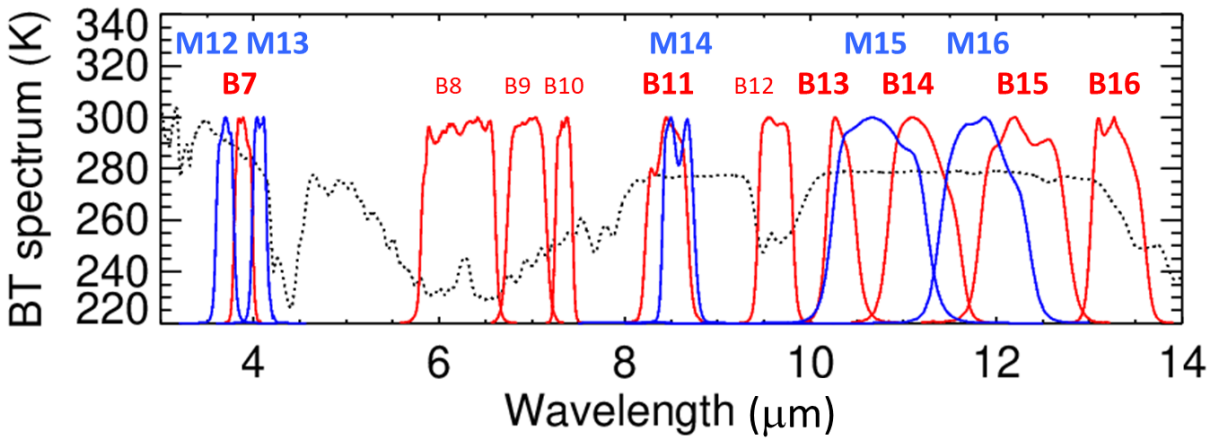

Figure 1. The MODTRAN-modeled BT spectrum for a typical ocean site (black dotted line) and the SRF for GOES17 ABI thermal bands (red) and SNPP VIIRS (blue).

Table 1. VIIRS and ABI spectral matched bands.

ABI/VIIRS Band	B7/M12	B7/M13	B11/M14	B13/M15	B14/M15	B14/M16	B15/M16
VIIRS center wavelength (μm)	3.70	4.05	8.55	10.76	10.76	12.01	12.01
ABI center wavelength (μm)	3.90	3.90	8.44	10.35	11.20	11.20	12.30

3.2 Site selection and cloud filtering

GOES16 is located over land at longitude of 75.2° West after operational, and GOES17 is over ocean at longitude of 137.2° West. The ocean sites along the strip on the image of Figure 2 can be used for GOES ABI and VIIRS comparison. The strips cover the ABI measurements with view angle up to 60 degrees. Applying the ray-matching method described in section 3.3, the large view angle coverage can have the assessment of view angle effect and RVS effect. It can also increase the comparison sample number for statical analysis. The strip selected for GOES17 are over ocean while the strip for GOES16 is over a mixed scenes of ocean, shore, and land. To enhance the comparison accuracy, the scene type and uniformity should be considered. This work focuses on the GOES17/ABI-VIIRS comparison and GOES17/ABI as reference for double difference.
Cloud cover also affects the scene uniformity and measurements with large view angle. The cloud cover over a scene can be identified using the ABI L2+ Binary Cloud Mask (BCM) product and VIIRS L2 BCM products. In this work, BCM-filtered clear sky measurement data are used for both VIIRS and ABI measurements.

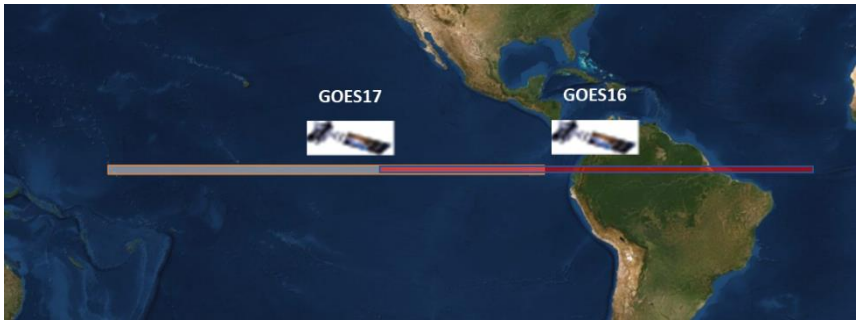

Figure 2. The site selection for ABI-VIIRS comparison. The gray color strip is the ocean site selected for GOES17/ABI and VIIRS comparison. The red strip includes ocean and land under GOES16.

3.3 View-angle-matching

Due to the satellite top of atmosphere (TOA) observations, the view angle difference influences the TEB measurements. The ray-matching method can reduce this effect when performing sensor comparisons [15]. TEB measurements are not sensitive to relative azimuth angle with sun. For the narrow strip selected over the ocean around GOES17 nadir as illustrated in Figure 2, we can have measurements with the same view zenith angle (VZA) of ABI and VIIRS. The measurements with same VZA and approximate same azimuth angle, are close to ray-matching. The pixels on one side of GOES17 nadir have the azimuth angle close to 90 degrees, while on the other side they are close to 270 degrees. The VIIRS measurements with the same VZA from the opposite direction (relative azimuth angle difference is close to 180 degree) can also be used for TEB comparison. The term quasi-ray-matching is used in this paper to refer to this kind of view angle matching, as illustrated in figure 3. It is noted that SNPP's and N20's orbit is not exactly perpendicular to the strip selected in Figure 2 and the azimuth difference is not exactly zero or 180 degrees. For TEB, it is not a significant effect on the comparison whether or not clear-sky measurements are used. In this work, we use both the ray-matching and quasi-ray-matching method to have more samples to be used for statistical analysis of the comparison between ABI and VIIRS. The measurement samples are collected and processed with VZA differences that are within 1 degree between ABI and VIIRS, considering VZA values up to 60 degrees.

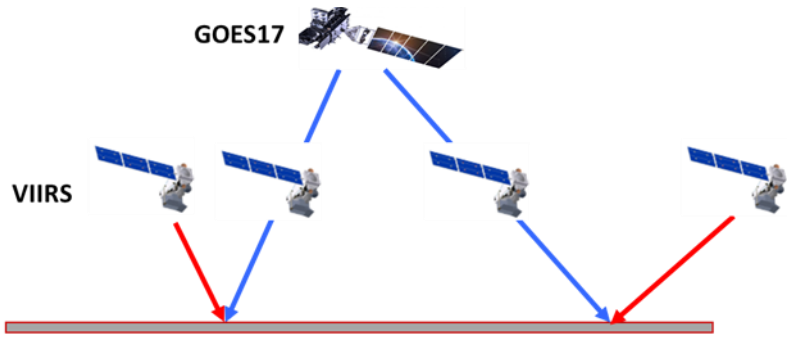

Figure. 3. Illustration of the ray-matching (blue rays) and quasi-ray-matching (red-blue rays) method. For ray-matching, the view zenith angles from the two instruments are the same view angle while their azimuth angle difference is close to zero. For quasi-ray-matching, the view zenith

angles from the two instruments are the same view angle while their azimuth angle difference is close to 180 degrees.

3.4 Simultaneous measurement and pixel-to-pixel comparison

In order to enhance the comparison accuracy for TEB, we only use nighttime observations. GOES17/ABI full disk images and VIIRS L1B and BCM products are used in this work. ABI full disk image is produced for every 10 minutes and the VIIRS granule with the nearest observation time is selected for the comparison. Considering the VIIRS 6-minutes granule in L1B data, the maximum observation time difference is less than 5 minutes.

The pixel size of ABI full disk image is 2 km for the TEB, while the VIIRS M band pixel size is 750m. There are two methods for the comparison of the selected site: (1) Average all pixels within the enclosed region of interest and then perform a BT comparison; (2) Resample the pixels within the enclosed region of interest from one of the instruments and then perform a pixel-to-pixel comparison. The first method is simpler, but may introduce additional uncertainties, especially for a large site. In this paper, a pixel-to-pixel comparison after resampling is used. The VIIRS measurement data are resampled to the ABI grid over the selected area. The pixel-to-pixel comparison after resampling enhances the comparison accuracy, by reducing the effects of nonuniformity and seasonal fluctuation. It also allows for the comparison to be performed over a broad range of BTs.

3.5 Data processing and statistical analysis

The data collected for comparison start on February 2019 after GOES17 ABI declared for operational. For the inter-comparison and stability trends of the TEB, the clear-sky measurements are processed and GOES17/ABI-SNPP/VIIRS and GOES17/ABI-N20/VIIRS pixel-to-pixel comparisons are analyzed separately. For the direct comparison, an entire year's (2020) comparison data are analyzed and for the trending all the monthly results from February 2019 to June 2022 are analyzed. The comparison uncertainty primarily comes from the uncertainty of each ABI and the uncertainty of the comparison method. Moreover, the comparison method uncertainty also includes the effects from ABI and VIIRS pixel geolocation uncertainty. If these uncertainties are assumed random, the total uncertainty should have a normal distribution of $\exp\left[-\frac{(x-x_0)^2}{2\sigma^2}\right]$, where x is the BT difference of the measurements over the scene, x_0 is the expected value of the BT difference from the measurements, and σ is the uncertainty of the expected value. Due to the scene dependency, this uncertainty assessment is for each site. The uncertainty of the comparison for each site can be estimated from the uncertainty propagation as: $\sigma_{ABI-VIIRS} = \sqrt{\sigma_{ABI}^2 + \sigma_{VIIRS}^2 + \sigma_{comparison}^2}$. The BT difference distribution between GOES17/ABI and VIIRS can be fitted using a Gaussian function. Hence, the BT difference and its uncertainty can be obtained from the regression of the comparison results and this modeling.

4 Comparison results

4.1 ABI-VIIRS comparison

All analyses shown in this section are for the matching bands over the selected ocean site with clear-sky nighttime measurements for the year 2020. The comparison is performed for pixel-to-pixel and simultaneous measurement. The differences in certain period of time are collected for statistical analysis. Using one year's worth of data reduces the seasonal fluctuations for comparison purposes. Figure 4 shows the ABI-VIIRS direct comparison results for the selected bands with view angle less than 10 degree around nadir. The histograms of the comparison differences between GOES17/ABI-SNPP/VIIRS and between GOES17/ABI-N20/VIIRS match well. Each of the histogram of their difference is fitted Gaussian function to derive the difference between ABI and VIIRS.

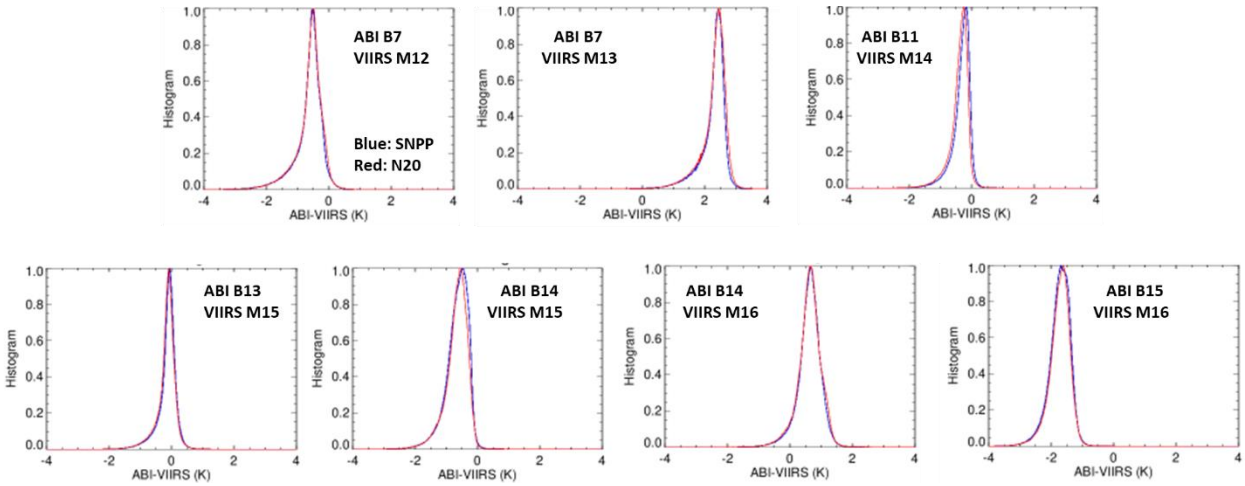

Figure. 4. The direct pixel-to-pixel and simultaneous GOES17/ABI-VIIRS comparison results for the matching band pairs over the ocean site for the year 2020. The blue curves define the histograms for the comparison with SNPP VIIRS, while the red curves represent the histograms for the comparison with N20 VIIRS.

4.2 SNPP/VIIRS and N20/VIIRS comparison

The double difference method is applied for SNPP/VIIRS and N20/VIIRS comparison. The pixel-to-pixel and simultaneous ABI-VIIRS comparison results for year 2020 presented in section 4.1 are used for double difference. Table 2 lists the ABI-VIIRS difference for SNPP and N20 and derived the difference between SNPP/VIIRS and N20/VIIRS for selected matching bands for year 2020. The large differences between ABI-VIIRS are due to the spectral mismatching and this effect is almost same for the comparison with SNPP/VIIRS and N20/VIIRS and can be basically canceled using the double difference. The ABI-VIIRS difference and derived the difference between SNPP/VIIRS and N20/VIIRS are listed in Table 2 for the matching band pairs. The differences between SNPP/VIIRS and N20/VIIRS are less than 0.1K for these bands. This result shows the consistent calibration and L1B measurements between SNPP VIIRS and N20/VIIRS TEB. In addition, ABI bands 13 and 14 are used as reference for SNPP/VIIRS and N20/VIIRS M15 comparison. The results, 0.027K and 0.021K difference, are remarkably close. Similarly,

VIIRS M16 also show the consistent results. It demonstrated the methodology feasibility for the bands without good spectral matching with ABI.

Table 2. SNPP/VIIRS and N20/VIIRS difference using double difference method.

ABI/VIIRS Band	B7/M12	B7/M13	B11/M14	B13/M15	B14/M15	B14/M16	B15/M16
G17/ABI-SNPP/VIIRS (K)	-0.510	2.422	-0.234	-0.059	-0.558	0.666	-1.668
G17/ABI-N20/VIIRS (K)	-0.501	2.439	-0.301	-0.086	-0.579	0.666	-1.671
SNPP/VIIRS-N20/VIIRS (K)	-0.009	-0.017	0.067	0.027	0.021	0.000	0.003

4.3 Stability assessment

The SNPP/VIIRS and N20/VIIRS differences presented in section 4.2 are for 2020 data. GOES17 ABI was declared operational on February 12, 2019, and the full disk L1B data has been available to the public since then. The use of GOES17/ABI as reference in this work starts from that date until the most recent date when the ABI and VIIRS L1B data and BCM products are publicly available. The GOES17/ABI-VIIRS differences are analyzed monthly for the trending.

Figure 5 displays the trending of monthly assessment of direct pixel-to-pixel and simultaneous GOES17/ABI-VIIRS comparison results for the matching band pairs. Each symbol is a processed difference over one month. Blue is for GOES17/ABI-SNPP/VIIRS comparison and red is for GOES17/ABI-N20/VIIRS comparison. As shown in Figure 1, even for a matching band pair, there are still spectral difference between ABI and VIIRS. This difference causes the difference in their BT measurements and these differences have seasonal variation. For ABI B7, VIIRS M15 and M16, two matching pairs for each have been used for comparison. The patterns of seasonal fluctuations are very different. These fluctuations are consistent for both ABI-SNPP/VIIRs and ABI-N20/VIIRS.

Figure 6 shows the trending of difference between SNPP/VIIRS and N20/VIIRS TEB using double difference. For VIIRS bands M15 and M16, there are two matched pairs for each of them and the difference between SNPP and N20 are derived for each matching pair. The fluctuations in the ABI-VIIRS differences are generally canceled. Due to the sample number effect in the statistical analysis, the uncertainties of monthly results are larger than that from yearly results. For these M bands, the differences between SNPP and N20 are generally within 0.2K.

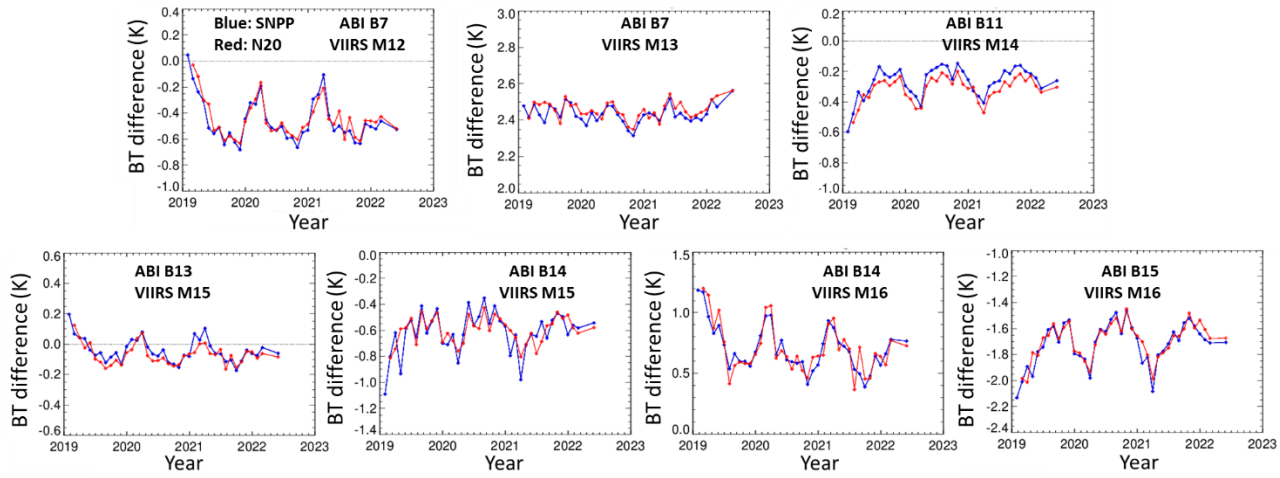

Figure. 5. The trending of direct pixel-to-pixel and simultaneous GOES17/ABI-VIIRS comparison results for the matching band pairs. Each symbol is a processed difference over one month. Blue is for GOES17/ABI-SNPP/VIIRS comparison and red is for GOES17/ABI-N20/VIIRS comparison.

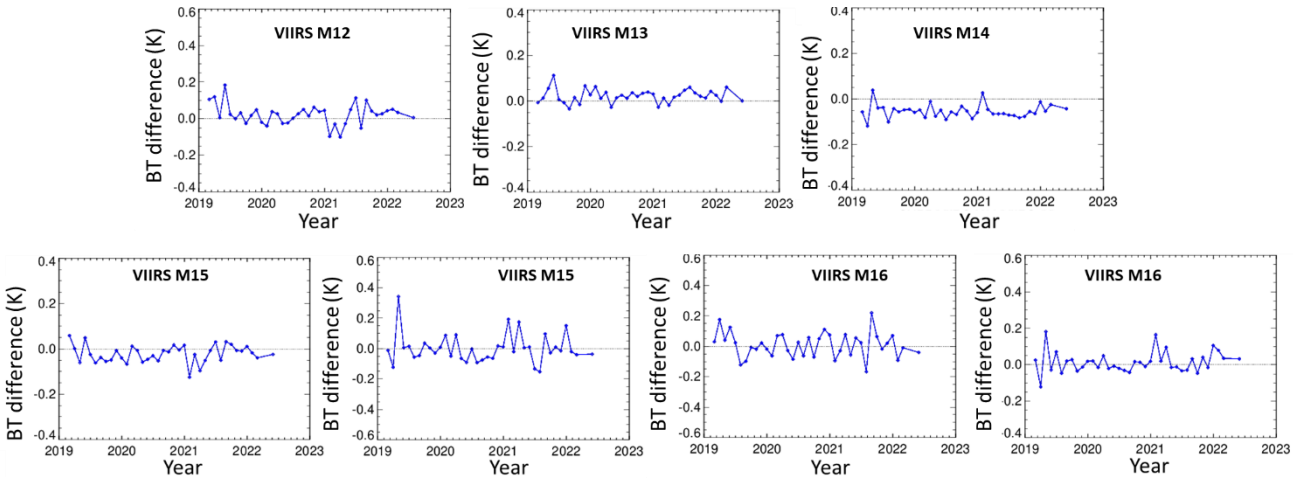

Figure. 6. The trending of difference between SNPP/VIIRS and N20/VIIRS TEB using double difference. Each symbol is a processed difference over one month.

4.4 View angle effect

The ABI-VIIRS difference and SNPP/VIIRS-N20/VIIRS comparison in sections 4.1 to 4.3 are the statistical analysis results using the measurements around the nadir. As a methodology assessment, the comparison difference vs view angle is analyzed. Figure 7 shows the difference between GOES17/ABI-SNPP/VIIRS and between GOES17/ABI-N20/VIIRS as function of ABI and VIIRS VZA. The VZA dependences are consistent between SNPP and N20 VIIRS. In general, the view angle dependence is not very significant for the differences between SNPP/VIIRS and N20/VIIRS. This result demonstrates the feasibility for GEO-LEO comparison with broad range of view angle.

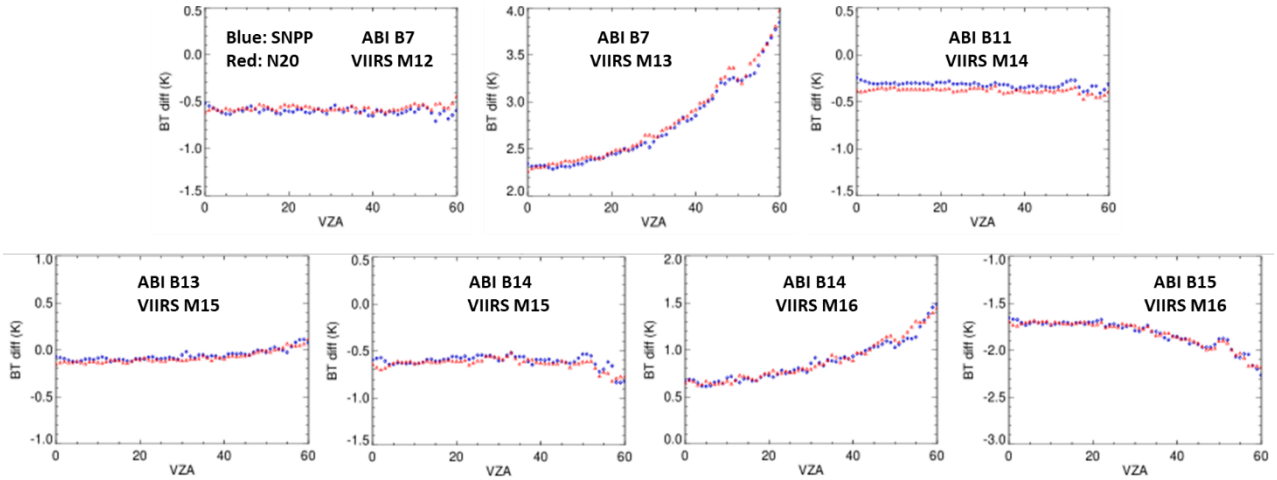

Figure. 7. The difference between GOES17/ABI-SNPP/VIIRS (blue) and between GOES17/ABI-N20/VIIRS (red) as function of ABI and VIIRS VZA.

In this work, the comparison samples are collected with ray-matching and quasi-ray-matching, as described in section 3.3 and Figure 2. In order to cover a VZA range up to 60 degrees over the selected strip in section 3.2, the orbits of SNPP and N20 are over a large range of longitudes and over both ocean and land. The VZA is defined as negative for the pixels on the west side of GOES17 nadir and positive for east side, in order to take the scene type at local time into consideration. Figure 8 shows the difference between GOES17/ABI-N20/VIIRS as function of ABI and VIIRS VZA. The difference between GOS17/ABI and SNPP/ABI has similar pattern and dependency. The results indicate that both the ray-matching and quasi-ray-matching have a consistent VZA dependency. This analysis demonstrates the use of quasi-ray-matching measurements for sensor inter-comparison and shows that the method can be applied GOES sensor measurements when ray-matching requirements are not available.

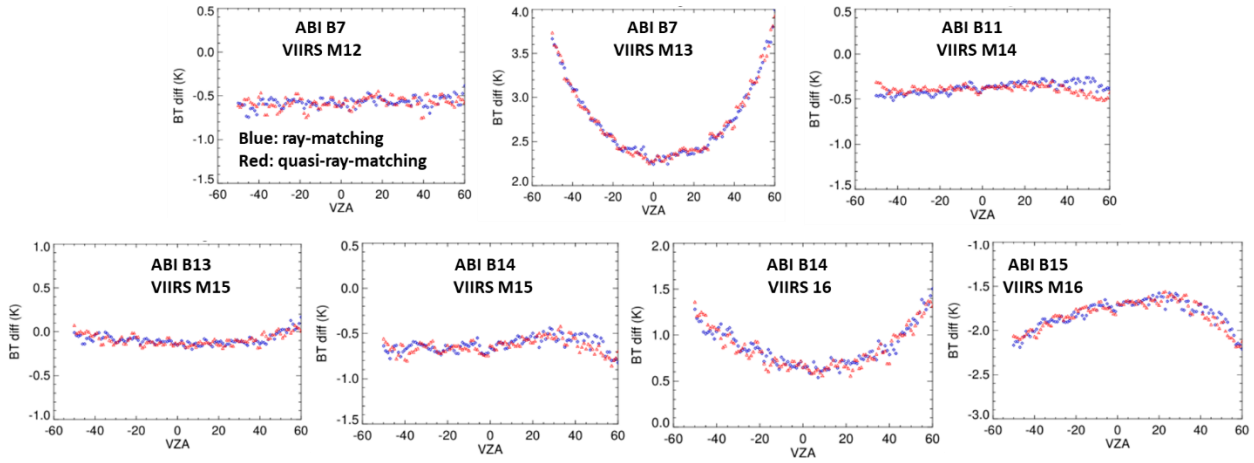

Figure. 8. The difference between GOES17/ABI-N20/VIIRS as function of ABI and VIIRS VZA. The blue symbols are their difference with ray-matching measurements and red symbols are for quasi-ray-matching.

5. Conclusion

The SNPP/VIIRS and N20/VIIRS TEB were compared using double differences, with GOES17/ABI as a reference. All the VIIRS M bands have been paired with one or two ABI bands. Although their spectral matching is not perfect, the spectral mismatching effect is generally canceled when applying a double difference comparison. A site over ocean around GOES17 nadir is selected for comparison. The site covers the GOES17/ABI view angle up to 60 degrees. Due to the mixture of ocean and land around GOES16 nadir, this paper focused on the use of GOES17/ABI as reference. The VIIRS M band pixels are resampled to ABI TEB pixel and pixel-to-pixel comparison is performed for all the comparison. ABI provides full disk measurements every 10 minutes and nearest VIIRS measurements are selected to achieve near simultaneous comparison. The nighttime clear-sky ABI and VIIRS measurements are processed from year 2019 to June 2022. Samples with view angle differences within 1 degree are collected and processed for comparison.

The GOES17/ABI-SNPP/VIIRS differences and GOES17/ABI-N20/VIIRS differences are used for double differences, from which the TEB differences between SNPP/VIIRS and N20/VIIRS are derived. Consistent measurements have been shown with differences smaller than 0.1K. The trending of ABI-VIIRS differences shows consistent seasonal fluctuation, with a dependency on the matching of band pairs. This effect is removed from the trending of SNPP-N20 differences. The SNPP-N20 difference is up to 0.2K, when examining the monthly trending. The view angle effect, including the comparison between ray-matching and quasi-ray-matching method are presented and discussed. The quasi-ray-matching method is demonstrated for the application to inter-sensor comparison.

References

1. C. Cao, F. Deluccia, X. Xiong, R. Wolfe, and F. Weng, " Early On-orbit Performance of the Visible Infrared Imaging Radiometer Suite (VIIRS) onboard the Suomi National Polar-orbiting Partnership (Suomi-NPP) Satellite", IEEE Transaction on Geoscience and Remote Sensing, DOI:10.1109/TGRS.2013.2247768, vol. 52, no. 2, pp1142 – 1156, 2014
2. X. Xiong, J. Butler, K. Chiang, B. Efremova, J. Fulbright, N. Lei, J. McIntire, H. Oudrari, J. Sun, Z. Wang, and A. Wu, "VIIRS on-orbit calibration methodology and performance", Journal Of Geophysical Research: Atmospheres, vol. 119, pp1–11, 2014
3. C. Cao et al., "NOAA-20 VIIRS on-orbit performance, data quality, and operational Cal/Val support," in Proceedings of SPIE, Nov. 2018, vol. 10781, p. 107810K, doi: 10.1117/12.2324329.
4. X. Xiong, H. Oudrari, J. McIntire, N. Lei, V. Chiang, and A. Angal, "Initial calibration activities and performance assessments of NOAA-20 VIIRS," in Proceedings of SPIE, Oct. 2018, p. 22, doi: 10.1117/12.2326897.
5. Cao, C., M. Weinreb, and H. Xu, "Predicting simultaneous nadir overpasses among polar-orbiting meteorological satellites for intersatellite calibration of radiometers", Journal of Atmospheric and Oceanic Technology, vol. 21, 537-542 (2004).
6. Gunshor, M. M., T. J. Schmit, D. R. Pogorzala, S. S. Lindstrom, J. P. Nelson, GOES-R series ABI Imagery artifacts, J. of Applied Remote Sensing, 14(3), 032411 (2020). [doi:10.1117/1.JRS.14.032411]

7. Schmit, T. J., Paul Griffith, Mathew M. Gunshor, Jaime M. Daniels, Steven J. Goodman, and William J. Lebai, "A Closer Look at the ABI on the GOES-R Series", Bulletin of the American Meteorological Society, 98 (4), 681-698 (2017)
8. Schmit, T. J., S. S. Lindstrom, J. J. Gerth, M. M. Gunshor, "Applications of the 16 spectral bands on the Advanced Baseline Imager (ABI)". J. Operational Meteor., 6 (4), 33-46 (2018). [doi: 10.15191/nwajom.2018.0604]
9. Goodman, S.J., T.J. Schmit, J. Daniels, W. Denig, K. Metcalf, "GOES: Past, Present, and Future", Reference Module in Earth Systems and Environmental Sciences, 1, 119-149 (2018)
10. Xiong, X., Wu, A. and Cao, C. On-orbit calibration and inter-comparison of Terra and Aqua MODIS surface temperature spectral bands. International Journal of Remote Sensing, 29: 5347–5359 (2008)
11. Chander, G., T. J. Hewison, N. Fox, X. Wu, X. Xiong, and W. J. Blackwell, "Overview of Intercalibration of Satellite Instruments", IEEE TRANSACTIONS ON GEOSCIENCE AND REMOTE SENSING, 51(3), 1056 (2013)
12. Yu, F. and X. Wu, Radiometric Inter-Calibration between Himawari-8 AHI and S-NPP VIIRS for the Solar Reflective Bands, Remote Sens. 8, 165 (2016). [doi:10.3390/rs8030165]
13. Li, Y., A. Wu, and X. Xiong (2013), Evaluating Calibration of MODIS Thermal Emissive Bands Using Infrared Atmospheric Sounding Interferometer Measurements, Proc. of SPIE Vol. 8724, doi: 10.1117/12.2016621
14. Chang, T., X. Xiong, G. R. Keller, and X. Wu, GEO-LEO reflective band intercomparison with bidirectional reflectance distribution function and atmospheric scattering corrections J. of Applied Remote Sensing, 12(1), 014002 (2018). [doi: 10.1117/1.JRS.12.014002]
15. Doelling, D., R. Bhatt, D. Morstad, B. Scarino. "Algorithm Theoretical Basis Document (ATBD) for ray-matching technique of calibrating GEO sensors with Aqua-MODIS for GSICS. (2011) http://gsics.atmos.umd.edu/pub/Development/AtbdCentral/GSICS_ATBD_RayMatch_NASA_2011_09.pdf